PROCEEDINGS B

rspb.royalsocietypublishing.org

Research

Cite this article: Swezey DS, Bean JR, Ninokawa AT, Hill TM, Gaylord B, Sanford E. 2017 Interactive effects of temperature, food and skeletal mineralogy mediate biological responses to ocean acidification in a widely distributed bryozoan. *Proc. R. Soc. B* **284**: 20162349.
http://dx.doi.org/10.1098/rspb.2016.2349

Received: 26 October 2016
Accepted: 20 March 2017

Subject Category:
Global change and conservation

Subject Areas:
ecology, physiology, biochemistry

Keywords:
calcification, global environmental change, magnesium regulation, phenotypic plasticity, bryozoan, colonial marine invertebrates

Author for correspondence:
Daniel S. Swezey
e-mail: dsswezey@ucdavis.edu

Electronic supplementary material is available online at https://dx.doi.org/10.6084/m9.figshare.c.3734401.

THE ROYAL SOCIETY PUBLISHING

Interactive effects of temperature, food and skeletal mineralogy mediate biological responses to ocean acidification in a widely distributed bryozoan

Daniel S. Swezey[1], Jessica R. Bean[2,4], Aaron T. Ninokawa[1], Tessa M. Hill[1,2], Brian Gaylord[1,3] and Eric Sanford[1,3]

[1]Bodega Marine Laboratory, University of California, Davis, 2099 Westshore Road, Bodega Bay, CA 94923, USA
[2]Department of Earth and Planetary Sciences, and [3]Department of Evolution and Ecology, University of California, Davis, One Shields Avenue, Davis, CA 95616, USA
[4]Museum of Paleontology, University of California, Berkeley, CA 94720-4780, USA

DSS, 0000-0003-2560-249X

Marine invertebrates with skeletons made of high-magnesium calcite may be especially susceptible to ocean acidification (OA) due to the elevated solubility of this form of calcium carbonate. However, skeletal composition can vary plastically within some species, and it is largely unknown how concurrent changes in multiple oceanographic parameters will interact to affect skeletal mineralogy, growth and vulnerability to future OA. We explored these interactive effects by culturing genetic clones of the bryozoan *Jellyella tuberculata* (formerly *Membranipora tuberculata*) under factorial combinations of dissolved carbon dioxide (CO_2), temperature and food concentrations. High CO_2 and cold temperature induced degeneration of zooids in colonies. However, colonies still maintained high growth efficiencies under these adverse conditions, indicating a compensatory trade-off whereby colonies degenerate more zooids under stress, redirecting energy to the growth and maintenance of new zooids. Low-food concentration and elevated temperatures also had interactive effects on skeletal mineralogy, resulting in skeletal calcite with higher concentrations of magnesium, which readily dissolved under high CO_2. For taxa that weakly regulate skeletal magnesium concentration, skeletal dissolution may be a more widespread phenomenon than is currently documented and is a growing concern as oceans continue to warm and acidify.

1. Introduction

Calcifying marine species use a variety of mineralogical forms or 'polymorphs' of $CaCO_3$ in skeletal material. These polymorphs include aragonite, calcite as well as calcite minerals containing high concentrations of magnesium (Mg). Many species incorporate more than one form of calcite into skeletal material [1–3]. The compositions of such biogenic calcites vary by taxonomic group and typical levels of Mg substitution into the crystalline lattice range from 0 to 20 mol% $MgCO_3$ [1]. In some species, the Mg content of skeletal calcite can be influenced by abiotic factors, including temperature, light and seawater carbonate saturation state among others [1,4,5]. As the Mg content of calcite increases, these materials become increasingly soluble and therefore more vulnerable to dissolution as seawater pH decreases [1–3].

Ocean absorption of global CO_2 emissions has reduced average surface water pH by at least 0.1 pH units since the beginning of the Industrial Revolution [6]. This process, termed ocean acidification (hereafter OA), is projected to accelerate in coming years, with a reduction of 0.3–0.5 pH units expected by 2100 [7]. Organisms secreting skeletons containing high-Mg calcite (i.e. exhibiting more than 12 mol% $MgCO_3$) may be particularly vulnerable to increasing

OA because of the kinetic sensitivity of this material to decreasing $CaCO_3$ saturation states in the global ocean [1–3]. Additionally, variation in the chemical and physical properties of biogenic calcites make Mg-dissolution relationships tenuous for some taxa, and chemical stability may not always be a simple function of Mg composition across all groups [1]. Taxa that secrete variable-Mg calcite skeletons in modern seas include for example, coralline algae, serpulid worms, foraminifera, echinoderms and a subset of bryozoan species among others [4].

Studies of the biological effects of OA suggest that environmental factors such as food availability [8,9] and warming [10,11] play critical roles in mediating the susceptibility of marine taxa to acidification. For example, plentiful food can offset the effects of OA [9,12], whereas increasing temperatures can either magnify [13] or ameliorate [14] its effects. There are many physiological mechanisms by which food and temperature might influence the susceptibility of marine organisms to acidification. Skeletal mineralogy is a plastic trait in some marine calcifiers [3], and mineralogy is known to vary with temperature [4,15], while overall calcification rates can be influenced by an animal's energetic state [16]. In this study, we investigate how mineralogical changes driven by both temperature and food availability interact to affect organismal vulnerability to OA.

(a) Ocean acidification in the California Current Large Marine Ecosystem

Along portions of the west coast of North America, wind stress patterns and near shore ocean circulation lead to the upwelling of deeper waters during spring and summer months that are naturally high in CO_2 and low in pH [17]. Intertidal and subtidal habitats exposed to these upwelled waters experience low saturation states with respect to aragonite and high-Mg calcite [17–19], and also experience significant spatial and temporal variation in temperature, plankton and nutrient concentrations [20]. This variation creates an alongshore mosaic of dynamic environmental conditions along large stretches of coastline. Furthermore, additional reductions in pH projected for surface waters in the California Current Large Marine Ecosystem (CCLME) due to increasing anthropogenic CO_2 emissions are among the most extreme expected for the World's oceans [21]. Models indicate that within as few as 30 years, atmospheric CO_2 inputs and altered oceanographic circulation could result in summer-long under-saturation with respect to aragonite and high-Mg calcite in the upper 60 m of the water column [21]. These changes have the potential to impact marine organisms that cannot tolerate extended exposure to low saturation states, with important implications for the ecology of the systems they inhabit [22].

(b) Study species

Bryozoans are a phylum of suspension-feeding colonial marine invertebrates, most of which calcify, with nearly 6000 described species found in benthic marine ecosystems throughout the world [23]. Bryozoans form colonies of genetically identical units termed zooids via asexual budding, and can be experimentally subdivided into clonal replicates and assigned to different treatments [24,25], allowing for experimental designs where variance components can be partitioned among genotypes. Skeletal mineralogy is a highly plastic trait in some bryozoan families, while in others, it appears more constrained [26–28]. Identifying environmental factors that influence skeletal Mg in a given clade can help determine which factors will exacerbate versus ameliorate the negative effects of OA.

Jellyella tuberculata (formerly *Membranipora tuberculata* [29]) is an encrusting cheilostome bryozoan typically found growing as an epibiont on macroalgae in low-intertidal and subtidal habitats in most of the World's temperate and tropical seas [29,30]. Along the west coast of Central and North America, this species ranges from Peru to northern California, USA. We used a six-month laboratory experiment to test how skeletal mineralogy and colony growth varies in *J. tuberculata* clones when exposed to projected changes in future ocean temperatures and carbonate chemistry, while simultaneously manipulating food availability. We hypothesized that growth and Mg content in lineages of bryozoan clones would decrease under elevated CO_2 and low $CaCO_3$ saturation states, but increase under warmer temperatures. We also expected increased food to buffer growth against the negative effects of high CO_2. Finally, we hypothesized that the interactive effects of warming temperature and high CO_2 would increase skeletal dissolution, whereas high food availability would reduce dissolution.

2. Material and methods

(a) Collections, cloning and culture protocol

Colonies of *J. tuberculata* were collected on intact blades of red algae from the low-intertidal zone at Dillon Beach, CA, USA (38°15′20.72 N, 122°58′15.63 W) during November 2013. Colonies were grown off of algal substrata onto acetate sheeting to provide a standardized substrate across all replicates, and were held for four months under pre-treatment conditions at Bodega Marine Laboratory (see the electronic supplementary material for further culturing methodology). While interactions between epiphytic bryozoan colonies and algal substrata are possible [31], examining such interactions was beyond the scope of this study. Colonies were propagated to produce eight replicate clones of each of eight genotypes, resulting in a total of 64 experimental colonies. One clone from each genetic replicate was then randomly assigned to each of the eight treatment combinations (see Experimental design). These colonies were cultured under approximately 350 µatm CO_2 at 16°C at high food concentrations and then photographed under a stereo microscope (Leica M125 with a Leica DC290 camera; Leica Microsystems, Wetzlar, Germany) prior to exposure to the experimental treatments (hereafter referred to as the treatment phase). Colonies were then photographed again at the completion of the eight-week treatment phase.

(b) Experimental design

Bryozoan colonies were cultured using a custom-designed flow-through OA system (see the electronic supplementary material) under a factorial combination of pCO_2 (approx. 385 µatm versus approx. 1050 µatm), temperature (11°C versus 21°C) and food (low versus high rations of cultured microalgae). Bryozoans in the high food treatment were fed an optimal concentration [32] of 200 cells μl^{-1} (100 µl *Rhodomonas* sp. + 100 µl *Isochrysis* sp.), whereas the low-food treatment received 25% of this amount (i.e. 25 µl *Rhodomonas* sp. + 25 µl *Isochrysis* sp.).

Temperatures and CO_2 values were chosen to represent typical high and low values encountered by *J. tuberculata* along the

California coast, ranging from non-upwelling summer conditions in southern California to upwelling conditions along the northern California coast [18,19,33]. We also report aragonite saturation state values of treatment seawater ($\Omega_{aragonite}$), a measure of the thermodynamic potential for this form of $CaCO_3$ to precipitate or dissolve in solution, which is dependent on both the temperature of seawater and dissolved Ca^{2+} and CO_3^{2-} concentrations. Because temperature-dependent solubility relationships for biogenic Mg-calcites are poorly resolved in most taxa due to carbonate and cation disordering [1], we use the established temperature-dependent solubility relationship of aragonite as a proxy for the solubility of *J. tuberculata* calcite. Recent syntheses have mapped the solubility of aragonite to the solubility of some biogenic high-Mg calcites with molar Mg to Ca ratios (Mg/Ca_C) of approximately 0.12–0.14 [2,3,34]. In this study, calcification with observed Mg/Ca_C at or exceeding 0.12 was therefore assumed to meet or exceed the solubility of aragonite, and hence be potentially susceptible to dissolution at $\Omega_{aragonite} \leq 1$.

(c) Skeletal magnesium analyses

We analysed the Mg content in skeletons of autozooids (feeding zooids) generated during the treatment phase (hereafter referred to as treatment phase zooids) in three to four colonies from each of our eight treatment groups. We also analysed the Mg content of zooids grown at 16°C during the pre-treatment phase (hereafter referred to as pre-treatment zooids) in one of these same colonies. The latter analysis was performed to compare the effects of treatments on the Mg content of calcification that was initially accreted during benign common garden conditions. This analysis was intended to provide information on how the Mg/Ca_C of calcification generated under one set of conditions may be affected by subsequent changes in conditions experienced by colonies.

Elemental analyses were carried out using an electron microprobe (Cameca SX-100, Gennevilliers, France). Bryozoan colonies from each treatment group were embedded in epoxy and finely polished to expose skeletal cross-sections for quantitative elemental spot analysis. Prior to and following each run, the instrument was calibrated using repeat measurements of calcite and celestine standards. Software (PeakSight 4.0) determined standard-based corrections were then applied to the data, and drift offsets subtracted. Average skeletal concentrations of Mg and Ca (mol%) were determined for two to five zooids in each colony by analysing an average of nine 1 µm spots (15 kV, 20 nA beam) distributed across both the centres and margins of the transverse lateral zooecial walls of each zooid (see the electronic supplementary material).

In total, Mg and Ca concentrations were measured from 103 zooids across treatment groups. Standard deviations in the reproducibility of each spot measurement were calculated via software algorithm (PeakSight v. 4.0) and experiment-wide error for elemental measurements was estimated as the standard deviation fraction of total concentration element recorded. This percentage was calculated for each measurement, and then averaged across the full dataset generating average error estimates for Mg and Ca observations of 1.8% and 1.4%, respectively. Statistical comparisons were performed on molar Mg/Ca_C of zooid calcite [3] using a linear mixed effects model implemented in JMP PRO 12 (see the electronic supplementary material for further detail). We further quantified the percentage of observed points in each zooid falling above Mg/Ca_C of 0.12 (and thus likely matching or exceeding the solubility of aragonite) to compare variation in the occurrence of elevated Mg/Ca_C among treatments.

To verify that dissolved Ca and Mg concentrations in our experimental containers did not differ significantly among treatment groups, we determined the dissolved concentrations of these metals in seawater from a random sample of experimental containers each week, using an inductively coupled plasma mass spectrometer to analyse seawater samples. See the electronic supplementary material for results and details on chemical monitoring during the experiment.

(d) Image and statistical analyses

From our photo record of colony development, we used image analysis software (ImageJ v. 1.48) to quantify the number of three ontogenetic stages in *J. tuberculata* colonies at the beginning and end of the eight-week treatment phase. Zooids were identified as (i) immature zooids (zooids that were still forming at the growing edges of colonies when the image was taken), (ii) feeding autozooids (with a gut and a well-developed lophophore possessing a full complement of tentacles), and (iii) degenerated autozooids (indicated by the breakdown of the lophophore and gut, leaving a darkened remnant of cells referred to as a brown body).

We statistically modelled the growth efficiency (GE) of colonies as $\log_{10}(N_n/N_a)$, where N_n is the number of new zooids of all types added during the treatment phase, and N_a is the number of feeding autozooids at the beginning of the treatment phase with temperature, CO_2 and food level treated as fixed factors in a mixed-model design implemented in JMP Pro 12 (see the electronic supplementary material for further model detail). GE represents a metric for growth productivity, accounting for the initial resource-generating 'population' of zooids [25]. We additionally modelled the number of new degenerated zooids observed in colonies, calculated by subtracting the number of degenerated zooids observed in colonies prior to treatment exposures from the number observed at the end of the treatment phase. To visualize this latter relationship, we regressed the number of new degenerated zooids observed in colonies against the number of new zooids added, comparing regression slopes across treatment groups. Challenging environmental conditions are thought to trigger the degeneration of active zooids as a means of energy conservation [35]. Thus, we interpret increases in the slope of this relationship (i.e. higher numbers of degenerated zooids observed relative to the numbers of new zooids generated) to indicate a compensatory trade-off, where growth of a colony is occurring at the expense of zooid function and/or longevity. While it is possible that some zooids degenerated and then re-generated during the course of the experiment, we assume that the patterns quantified from images taken at the beginning and end of the experiment are an accurate reflection of compensatory shifts that occurred throughout this period.

The dissolution of zooid calcification during the study was apparent in our photo record. In this species, mature zooids typically possess large prominent calcified structures (termed tubercles, see electronic supplementary material, figure S1). Using our photo records of colony growth, we randomly selected 30 pre-treatment zooids and 30 mature treatment phase zooids from each colony used in our skeletal magnesium analysis. For each zooid, we recorded whether its surface exhibited: (i) no observable dissolution, (ii) active dissolution as indicated by pitting and depressions in calcified structures, or (iii) the disappearance of tubercle calcification under strong dissolution (electronic supplementary material, figure S1). We then compared dissolution of these colonies in separate analyses for zooids generated during the pre-treatment and the treatment phases using a linear mixed effects model (JMP PRO v. 12).

3. Results

(a) Saturation state

Aragonite saturation states differed significantly among our temperature × CO_2 treatments (one-way analysis of variance (ANOVA), $F_{3,279} = 1599.75$, $p < 0.0001$). The low CO_2

treatments had a mean $\Omega_{aragonite}$ of 2.37 (s.d. = 0.18) and 2.49 (s.d. = 0.23) at 11°C and 21°C, respectively, whereas the high CO_2 treatments had mean values of 0.99 (s.d. = 0.07) and 1.08 (s.d. = 0.08) at 11°C and 21°C, respectively. See electronic supplementary material for additional chemistry results.

(b) Initial condition of bryozoan colonies

At the beginning of the treatment phase, there were no significant differences in the total number of zooids among colonies assigned to each of the eight treatment combinations (one-way ANOVA, $F_{7,63} = 1.402$, $p = 0.223$), nor were there differences in the proportion of degenerated versus active zooids (one-way ANOVA, $F_{7,63} = 0.701$, $p = 0.670$). Zooids generated prior to the treatment phase did not exhibit signs of dissolution.

(c) Growth efficiency and colony degeneration

GE increased with elevated food ($p = 0.007$), but GE was not significantly affected by temperature, CO_2 or interactions among these factors (figure 1*a*). Variance components associated with genotype explained 38.82% of total variance in the GE model; however, no significant differences were observed among genotypes.

The number of newly degenerated zooids increased with the number of new zooids added during the treatment phase ($p < 0.0001$) and increased under colder temperature ($p = 0.013$; figure 1*b*). Zooid degeneration also varied with the interaction terms of temperature × new zooids ($p < 0.0001$), CO_2 × new zooids ($p = 0.006$) and the four-way interaction of temperature × CO_2 × food × new zooids ($p = 0.009$). The slope of the relationship between new degenerated zooids and new zooids added was significantly higher at 11°C, high food, high CO_2 when compared with the majority of colonies held at 21°C and when compared with colonies held under 11°C, high food, low CO_2 (figure 1*b*).

(d) Skeletal Mg/Ca

Individual measurements of zooid Mg/Ca_C ranged from 0 to 0.218 across treatments (figure 2) with Mg/Ca_C averaging 0.099 (s.d. = 0.024), 0.114 (s.d. = 0.033) and 0.134 (s.d. = 0.035) in zooids added at 11°C, 16°C and 21°C, respectively, under low CO_2, high food conditions (see electronic supplementary material, figure S2 and table S2). Variability in Mg/Ca_C measurements in zooids within treatment groups was large and well above instrumental error, with standard deviations ranging from 20% to 56% of mean (electronic supplementary material, table S2), indicating that *J. tuberculata* zooids are composed of a highly variable Mg calcite.

Despite this naturally occurring variation, strong differences in the skeletal mineralogy of treatment phase zooids were observed between temperature treatments ($p < 0.0001$), with zooids exhibiting 29% greater Mg/Ca_C at 21°C ($\mu = 0.130$) compared with zooids cultured at 11°C under low CO_2 conditions ($\mu = 0.101$). Mg/Ca_C of treatment phase zooids within each temperature group did not differ across food or CO_2 levels (figure 2*b*). The occurrence of measurements containing Mg/Ca_C in excess of 0.12 (likely corresponding to equivalent or higher solubility than aragonite) was 169% greater in new zooids grown at 21°C compared with 11°C ($p < 0.0001$, figure 3*a*), with 65% of Mg/Ca_C measurements falling at or above 0.12 at 21°C. Mg/Ca_C in pre-treatment zooids varied with exposure to treatment phase temperature ($p = 0.001$), treatment phase CO_2 ($p = 0.045$), the interaction of treatment phase temperature × CO_2 ($p = 0.016$) and the three-way interaction of treatment temperature × CO_2 × food level ($p = 0.031$). Pre-treatment zooids exposed to high CO_2 and low food at 11°C exhibited a 32.5% decrease in the mean Mg/Ca_C ($p = 0.022$) compared with the low CO_2, low-food treatment at 11°C, with the mean Mg/Ca_C being reduced from 0.12 to 0.081. Pre-treatment zooids exposed to high CO_2 and low food at 11°C also exhibited lower Mg/Ca_C when compared with all pre-treatment zooids exposed to 21°C (figure 2*a*; see electronic supplementary material, table S3 for means comparisons and full model output).

$Mg/Ca_C > 0.12$ varied in pre-treatment zooids with treatment phase temperature ($p = 0.005$), the interaction of treatment phase temperature × treatment phase CO_2 ($p = 0.054$) and with the three-way interaction of treatment phase temperature × CO_2 × food ($p = 0.040$). The occurrence of $Mg/Ca_C > 0.12$ was 86% lower in pre-treatment zooids exposed to high CO_2 and low food at 11°C when compared with pre-treatment zooids exposed to high CO_2 with low food at 21°C ($p = 0.047$).

(e) Skeletal dissolution

Dissolution of treatment phase zooids was greater at higher temperature ($p < 0.0001$) and elevated CO_2 ($p < 0.0001$), and varied with the interactions of temperature × CO_2 ($p < 0.0001$), and temperature × food ($p < 0.0001$), as well as with the three-way interaction of temperature × CO_2 × food ($p < 0.0001$; figure 3*b*). Dissolution was not observed in zooids held under low CO_2. At 21°C/high CO_2, 90.6% and 92.6% of zooids exhibited dissolution for low and high food groups, respectively. At 11°C/high CO_2, 41% and 9.7% of zooids exhibited dissolution for low and high food groups, respectively (figure 3*b*). Under this treatment combination, there was suggestive evidence that the frequency of dissolution was higher under low-food conditions than high food ($p = 0.077$).

Dissolution of pre-treatment zooids was greater when colonies were exposed to high versus low CO_2 conditions during the treatment phase ($p < 0.0001$). Treatment phase temperatures and food levels did not cause significant differences in the dissolution of pre-treatment zooids under high CO_2 (figure 3*b*). Under high CO_2 at 11°C, 98.9% and 87.1% or pre-treatment zooids exhibited dissolution under low and high food, respectively, compared with 97.7% and 96.6% at low and high food under 21°C treatments.

4. Discussion

In this study, we hypothesized that multiple oceanographic parameters would interact to affect the growth and skeletal mineralogy of the bryozoan *J. tuberculata*, a colonial marine invertebrate with a global geographical distribution that includes all of the World's warmer seas. Surprisingly, bryozoan clones maintained equivalent growth efficiencies across treatments, even under the combination of conditions that we expected to be stressful (cold temperatures and high CO_2). However, this maintenance was associated with costs to zooid longevity, with greater zooid degeneration relative to the production of new zooids (figure 1*b*). This

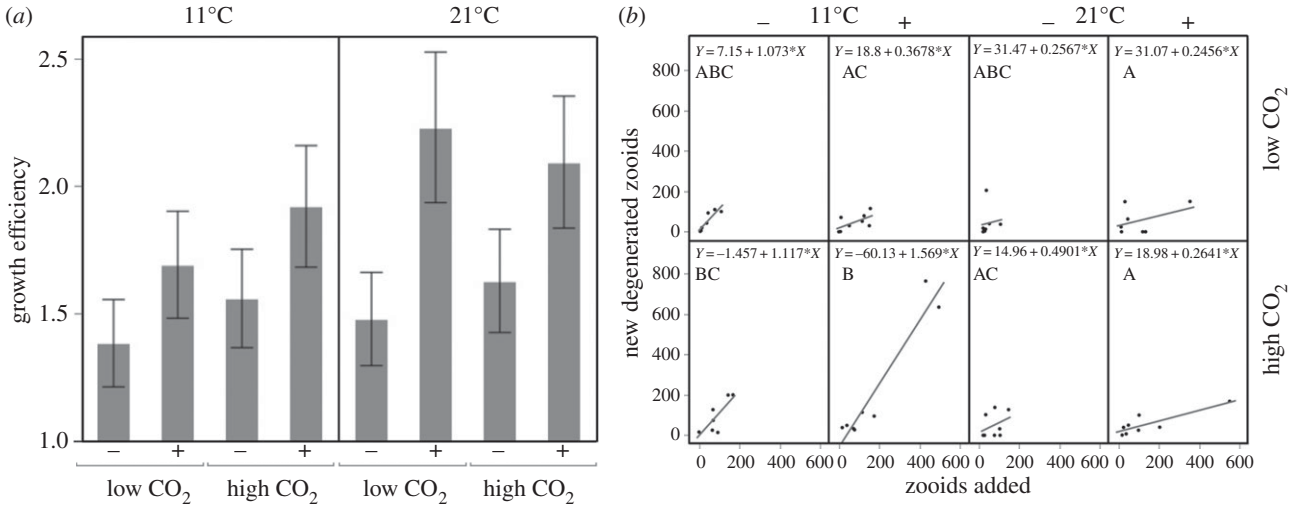

Figure 1. Growth efficiency (GE) and the number of new degenerated zooids relative to new zooids added in colonies. (*a*) Elevated food increased GE across treatment groups ($p = 0.007$), but GE was found to be equivalent across temperature and CO_2 levels. Error bars are ± 1 s.e. (*b*) The number of new degenerated zooids observed relative to the number of new zooids added by colonies increased under cold temperatures ($p < 0.0001$), high CO_2 ($p = 0.006$) and the interaction of temperature $\times$ CO_2 $\times$ food $\times$ new zooids added ($p = 0.009$). Shared letters indicate slope relationships among treatment groups that are not significantly different from each other ($p > 0.05$). This pattern suggests that colonies are able to maintain equivalent growth efficiencies across a range of conditions by increasing the degeneration of autozooids and redirecting this energy to the growth of new zooids.

degeneration decreased in warm temperatures, concurrent with an increase in the mean GE (figure 1*a*). These results suggest that growth is supported in adverse environments (e.g. cold temperatures accompanied by high CO_2) by an increase in polypide (lophophore and visceral mass) degeneration of existing zooids, with colonies translocating limited available energy from maintenance functions to support the production and development of new zooids [23,35,36].

Jellyella tuberculata exhibited striking dissolution under dissolved CO_2 concentrations that are already experienced episodically by this species in the northern portion of its geographical range on the California coast during upwelling events. These conditions are expected to become increasingly common under projected global CO_2 emissions scenarios [21]. However, we found that dissolution was also strongly modulated by temperature and food availability, which affect skeletal Mg content of this species. The amount of Mg incorporated into skeletal material appears to be weakly regulated in *J. tuberculata*, potentially reflecting the evolution of a generalist growth and calcification strategy in this species, and the family Membraniporidae more broadly, which may render it more vulnerable to OA than other taxa (see below for further discussion).

(a) High temperature and low-food exacerbate dissolution

Jellyella tuberculata appears to secrete a highly heterogeneous mixture of Mg calcite, indicated by the range of Mg/Ca_C observed among and within zooids sampled in this study. During the course of this study, the skeletal mineralogies of three zooids from a field-collected colony were analysed using the same methods applied to our experimental colonies. These results also indicated the presence of variable Mg calcite, with Mg/Ca_C measurements within and among zooids ranging from 0.111 to 0.160 (Swezey *et al.*, unpublished data), consistent with our laboratory findings and indicating that our results are likely representative of natural trends in *J. tuberculata* calcite from the California coast. Because instrumental error was low throughout our analysis, this variation appears to be a feature of this and potentially other high-Mg secreting species. Within this natural variation, Mg/Ca_C increased with temperature (figures 2*b* and 3*a*), supporting latitudinal trends observed previously in some bryozoans [27].

We also observed an increase in the dissolution of zooids grown in our high temperature treatments (figure 3*b*). We surmise that this pattern is primarily driven by the formation of high-Mg calcite at warm temperatures, which is then susceptible to subsequent dissolution under high CO_2. In our experiment, the mean aragonite saturation state was roughly equivalent across high CO_2 treatments ($\Omega_{arag} = 0.997$ and $\Omega_{arag} = 1.082$ for 11°C and 21°C), yet we saw marked dissolution under 21°C when compared with 11°C. This trend suggests that an increase in the Mg content of zooids grown in the high temperature treatments was a dominant cause of skeletal dissolution observed in our experiment.

In addition to Mg/Ca_C changes associated with temperature, colonies in our low-temperature, low-food treatments exhibited elevated mean Mg/Ca_C and elevated $Mg/Ca_C > 0.12$ in both pre-treatment and treatment phase zooids added under low CO_2 when compared with colonies receiving high food (figures 2 and 3*a*). While these trends were not statistically significant, they indicate that Mg regulation is likely under some level of metabolic control in this species, whereby colonies with an elevated energetic status are more capable of excluding Mg ions from the calcite lattice. Low-food clones held under high CO_2 at 11°C exhibited a roughly fourfold increase in the frequency of dissolution of treatment phase zooids and a 12% increase in dissolution of pre-treatment zooids, compared with colonies from the high CO_2, 11°C, high food group (figure 3*b*). This difference is likely driven by increasing Mg concentrations in skeletal calcite, but may also reflect a more general disruption of skeletal maintenance when food and energy are limited. This food effect was not apparent in 21°C treatments, where $Mg/Ca_C > 0.12$ and dissolution under high CO_2 was elevated in all groups.

Morse *et al.* [1] noted that rising pCO_2 should result in sequential dissolution of Mg calcite according to mineral

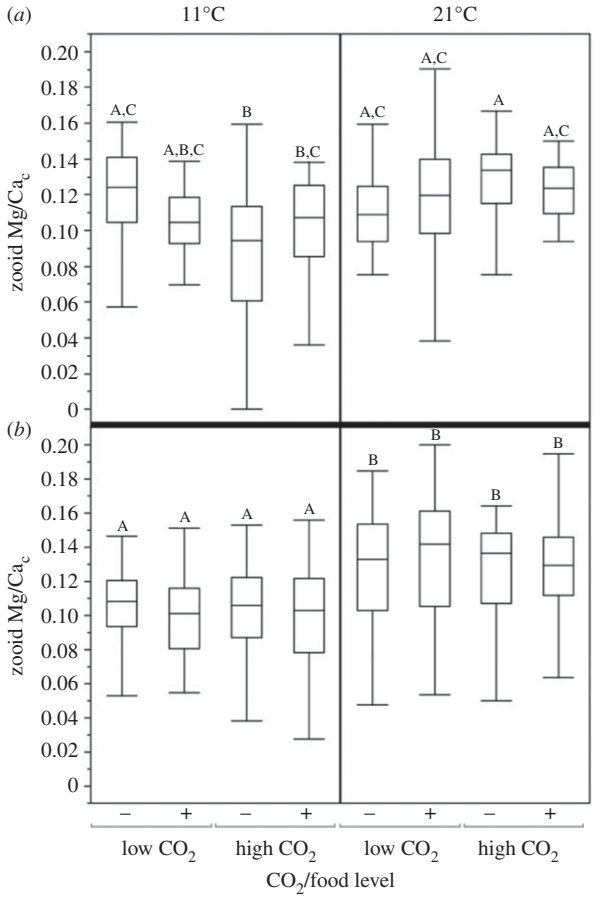

Figure 2. Box plots of Mg/Ca_C in bryozoan zooids exposed to experimental treatments. +/− indicate high and low-food groups, respectively. (*a*) Mg/Ca_C ratios in pre-treatment zooids initially generated under 16°C low CO_2, but then subsequently exposed to altered temperatures, CO_2 and food concentrations. Reduced Mg/Ca_C is observed under high CO_2 in pre-treatment zooids exposed to 11°C and low-food concentrations. (*b*) Mg/Ca_C ratios in zooids generated during the treatment phase. Elevated Mg/Ca_C is observed in new zooids added under 21°C compared with 11°C. Shared letters indicate groups that are not significantly different from each other based on means comparisons of least-squares group estimates ($p > 0.05$) in separate analyses for pre-treatment and treatment phase zooids.

stability, gradually leading to removal of the more soluble phases until the least soluble phases remain. Despite our observations of extensive dissolution under high CO_2, significant reductions in the average Mg/Ca_C of zooids only occurred in pre-treatment zooids exposed to high CO_2 and low food when colonies were held at 11°C, but not when exposed to 21°C (figure 2*a*). This pattern suggests that at 21°C, *J. tuberculata* may exhibit elevated calcification activity, continuing to biomineralize in the face of dissolution. By contrast, colonies exposed to high CO_2 and low food do not appear to replace lost high-Mg calcite in pre-treatment zooids when held at 11°C. This outcome may reflect a diversion of investment from reparative calcification to new zooid growth under these strenuous conditions, leading to predicted sequential dissolution and reductions in Mg/Ca_C over time.

(b) Taxonomic patterns of mineralogical control

Bryozoans employ a broad array of mineralogical strategies, and occupy 63% of the theoretically estimated space available for biomineralization, a dimensionless calculation of how widely a group varies in skeletal composition relative to the total range of known mineralogical strategies available to calcifying species (see [26] for details on calculation). Relative to other bryozoan families that occupy an average of 11% of this total range, Membraniporidae has among the most variable skeletal compositions, occupying approximately 87% of the range calculated for all bryozoan taxa [26]. Values of 14 mol% $MgCO_3$ have been recorded in *J. tuberculata* from Bermuda [37], where 21°C is a frequent sea surface temperature experienced in near shore habitats [38]. These $MgCO_3$ values are among the highest recorded in all bryozoan taxa [27].

Why is mineralogical composition so variable both within and among species in this family compared with nearly all other bryozoan taxa? Unlike most bryozoan taxa, members of this family possess a broadly dispersing cyphonautes larval form, spending two weeks to two months in the plankton [29,39], with concomitant high levels of genetic connectivity and a cosmopolitan global distribution [29,30,40]. Broad dispersal across multiple environments may therefore have selected for high levels of plasticity in skeletal mineralogy under spatially variable conditions. Adult colonies of the Membraniporidae also exhibit extremely rapid growth rates relative to other clades [23,41] and are dominant competitors for space on ephemeral habitat [23,42]. At our Dillon Beach collection site, this species consistently overgrows all other locally occurring encrusting bryozoan species (D.S.S. *et al*. 2013, personal observation). Rapid growth rates associated with this competitive dominance may have selected for reduced regulatory investment in calcite homogeneity and stability in favour of accelerated growth under a variety of environmental conditions. Indeed, this species maintains high growth rates even under adverse conditions at the expense of zooid (and potentially eventual colony) longevity. These hypothesized trade-offs among growth, longevity and plasticity in skeletal mineralogy might also lead to pronounced dissolution and morphological changes under increasing temperature and dissolved CO_2 concentrations.

(c) Vulnerability in a coastal upwelling region

To the best of our knowledge, *J. tuberculata* does not occur along the California coast north of our study region of Bodega Bay ([30], D.S.S. *et al*. 2013, personal observation). Areas north of this location have been identified as centres of persistent coastal upwelling, where cold, low saturation state conditions prevail during the spring and summer months [17–19]. Our results suggest that *J. tuberculata* is mismatched with conditions in the upwelling zone of northern California. We hypothesize that *J. tuberculata* weakly regulates mineralogical composition, which may limit its northern distribution to Bodega Bay and locales south, and render this species more vulnerable to changing ocean conditions. In the case of *J. tuberculata*, temperatures and phytoplankton concentrations that prevail before the seasonal onset of upwelling may determine how susceptible colonies will be to dissolution when exposed to corrosive waters. Dissolution of skeletal material under recently intensified upwelling conditions along the west coast of North America has occurred in other taxa (e.g. pteropods; [43]), and consistent with our laboratory results, *J. tuberculata* colonies exhibit signs of skeletal dissolution in the field during periods of

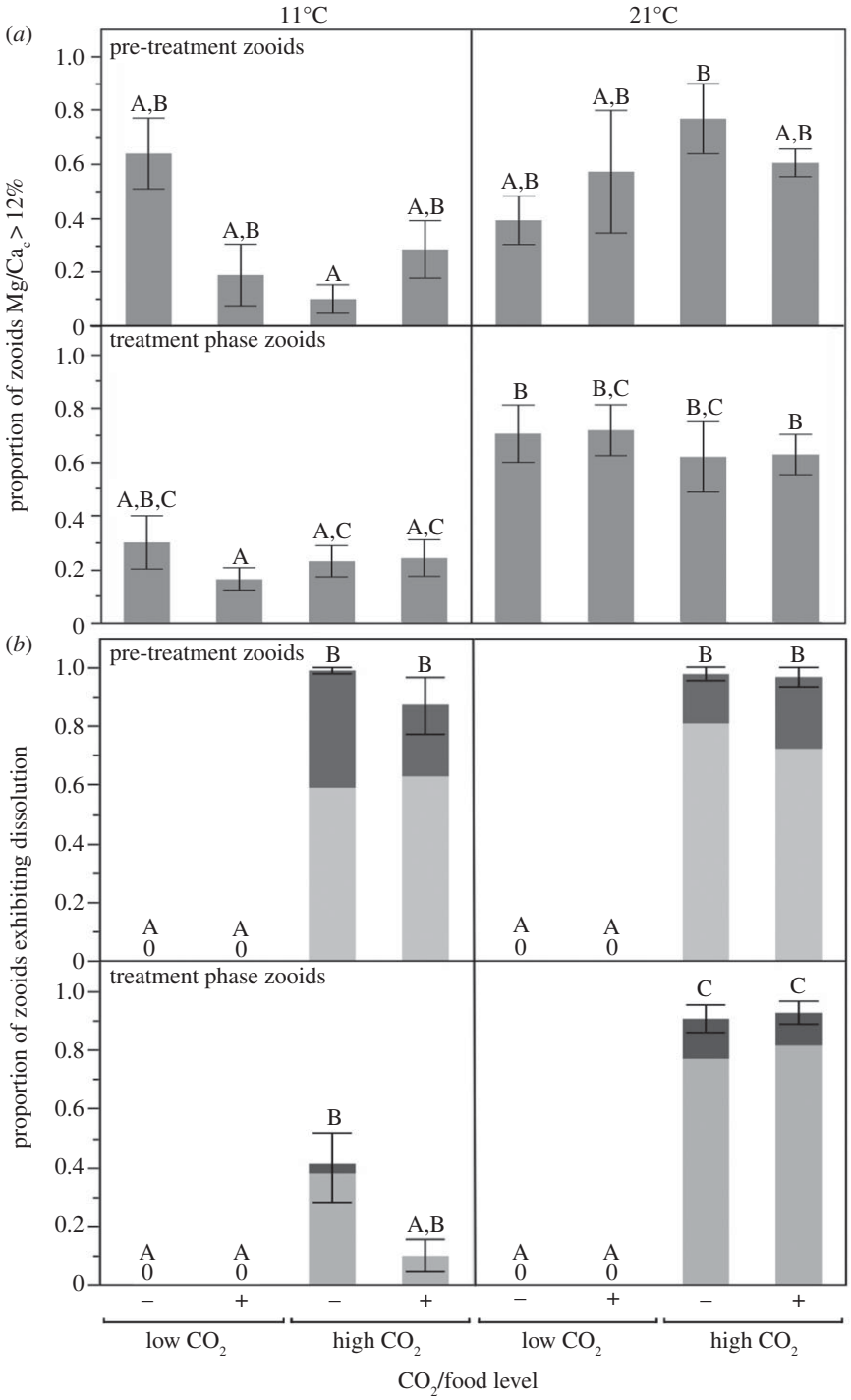

Figure 3. Dissolution of zooids in relation to the presence of high-Mg calcite. Top boxes in (*a*) and (*b*) show differences in pre-treatment zooids generated under 16°C low CO_2 and then subsequently exposed to altered temperatures, CO_2 and food concentrations. Lower panels show differences in zooids generated under the treatment conditions. +/− indicate high and low-food groups, respectively. Shared letters indicate groups that are not significantly different from each other based on means comparisons of least-squares group estimates ($p > 0.05$) in separate analyses for pre-treatment (upper boxes) and treatment phase (lower boxes) zooids. (*a*) Mean percentage (±1 s.e.) of measurements falling above $Mg/Ca_C = 0.12$ (approximate aragonite solubility) in zooids under treatment conditions. Uniformly elevated Mg calcite is observed at 21°C. At 11°C, low CO_2, low food, elevated Mg calcite is observed, potentially leading to elevated dissolution under high CO_2. (*b*) Mean percentage (±1 s.e.) of colonies exhibiting dissolution under experimental treatments. Darker shades represent the mean proportion of zooids exhibiting complete tubercle dissolution and lighter shades indicate proportions exhibiting partial dissolution. Pre-treatment zooids generated under 16°C showed similar dissolution levels as new zooid generated at 21°C, while a reduction in dissolution is observed in zooids generated at 11°C.

upwelling activity at Dillon Beach (D.S.S. *et al*. 2013, personal observation)

Observations and model projections suggest that climate change will increase the intensity of coastal upwelling in temperate latitudes [44–46], where upwelling seasons are projected to start earlier and end later [46]. Conversely, separate analyses have indicated that increased heat budgets due to elevated greenhouse gas concentrations may enhance stratification in the California Current System, deepening the thermocline and leading to higher temperatures in coastal waters [47,48]. Near shore habitats of coastal California have experienced significant warming in recent years [49,50] and alternations between warming and upwelling conditions [51] may deleteriously interact with the stability of calcification of some marine invertebrate species.

Skeletal dissolution in organisms that loosely regulate the Mg content of their calcified structures may be a widespread phenomenon that plays an important and underappreciated role in mediating the effects of OA. Reduced calcification rates and shifts in competitive hierarchies have been observed in other high-Mg calcite-secreting species such as coralline algae, concurrent with increasing OA [52]. Large-scale ecological impacts may therefore already be underway for some benthic marine communities. Quantifying the interactive effects of temperature, food availability and CO_2 on growth and skeletal mineralogy in other potentially vulnerable high-Mg taxa should be a priority for future research.

Authors' contributions. D.S.S., J.R.B. and E.S. conceived the study, and all authors contributed to its design. D.S.S., J.R.B. and A.T.N. conducted the experiments and carried out analyses of water chemistry, the latter with input from T.M.H. D.S.S. conducted the statistical analyses, and all authors participated in the interpretation of data. D.S.S. and E.S. drafted the manuscript, and all authors contributed significantly to revisions. All authors gave final approval for publication.

Competing interests. We declare we have no competing interests.

Funding. This work was supported by grant nos. OCE-0927255, OCE-1041089, OCE-1220648 and DGE-0841297 from the National Science Foundation and the University of California Multicampus Research Programs and Initiatives (MRPI). D.S.S. was also supported by an NSF Graduate Research Fellowship.

Acknowledgements. We would like to thank G. Baxter, N. Botto, M. Carroll, K. Griffith, D. Hall, L. Heidenreich, T. Landers, J. Lankford, K. Laughlin, J. Newman, S. Roeske, L. Rose, N. Sippl-Swezey, P. Stull and T. Woods for their help with field and laboratory work and analyses during the course of this project. We would also like to thank N. Willits for statistical advice. This manuscript was improved by helpful comments from J. Stachowicz, R. Grosberg and two anonymous reviewers.

References

1. Morse JW, Andersson AJ, Mackenzie FT. 2006 Initial responses of carbonate-rich shelf sediments to rising atmospheric pCO_2 and 'ocean acidification': role of high Mg-calcites. *Geochim. Cosmochim. Acta* **70**, 5814–5830. (doi:10.1016/j.gca.2006.08.017)
2. Andersson AJ, Mackenzie FT, Bates NR. 2008 Life on the margin: implications of ocean acidification on Mg-calcite, high latitude and cold-water marine calcifiers. *Mar. Ecol. Prog. Ser.* **373**, 265–273. (doi:10.3354/meps07639)
3. Ries JB. 2011 Skeletal mineralogy in a high-CO_2 world. *J. Exp. Mar. Biol. Ecol.* **403**, 54–64. (doi:10.1016/j.jembe.2011.04.006)
4. Chave KE. 1954 Aspects of the biogeochemistry of magnesium, 1. Calcareous marine organisms. *J. Geol.* **62**, 266–283. (doi:10.1086/626162)
5. Mackenzie FT, Bischoff WD, Bishop FC, Loijens M, Schoonmaker J, Wollast R. 1983 Magnesian calcites: low temperature occurrence, solubility and solid-solution behavior. In *Carbonates: mineralogy and chemistry*, pp. 97–144. Washington, DC: Mineralogical Society of America.
6. Orr *et al.* 2005 Anthropogenic ocean acidification over the twenty-first century and its impact on calcifying organisms. *Nature* **437**, 681–686.
7. Caldeira K, Wickett ME. 2005 Ocean model predictions of chemistry changes from carbon dioxide emissions to the atmosphere and ocean. *J. Geophys. Res. Oceans* **110**, 405. (doi:10.1029/2004JC002671)
8. Cohen AL, Holcomb M. 2009 Why corals care about ocean acidification: uncovering the mechanism. *Oceanography* **22**, 118–127. (doi:10.5670/oceanog.2009.102)
9. Thomsen J, Casties I, Pansch C, Körtzinger A, Melzner F. 2013 Food availability outweighs ocean acidification effects in juvenile *Mytilus edulis*: laboratory and field experiments. *Glob. Change Biol.* **19**, 1017–1027. (doi:10.1111/gcb.12109)
10. Kroeker KJ, Kordas RL, Crim R, Hendriks IE, Ramajo L, Singh GS, Duarte CM, Gattuso J-P. 2013 Impacts of ocean acidification on marine organisms: quantifying sensitivities and interaction with warming. *Glob. Change Biol.* **19**, 1884–1896. (doi:10.1111/gcb.12179)
11. Byrne M. 2011 Impact of ocean warming and ocean acidification on marine invertebrate life history stages: vulnerabilities and potential for persistence in a changing ocean. *Oceanogr. Mar. Biol.* **49**, 1–42. (doi:10.1201/b11009-2)
12. McCulloch M, Falter J, Trotter J, Montagna P. 2012 Coral resilience to ocean acidification and global warming through pH up-regulation. *Nat. Clim. Change* **2**, 623–627. (doi:10.1038/nclimate1473)
13. Anthony KRN, Kline DI, Diaz-Pulido G, Dove S, Hoegh-Guldberg O. 2008 Ocean acidification causes bleaching and productivity loss in coral reef builders. *Proc. Natl Acad. Sci. USA* **105**, 17 442–17 446. (doi:10.1073/pnas.0804478105)
14. Kroeker KJ, Gaylord B, Hill TM, Hosfelt JD, Miller SH, Sanford E. 2014 The role of temperature in determining species' vulnerability to ocean acidification: a case study using *Mytilus galloprovincialis*. *PLoS ONE* **9**, e100353. (doi:10.1371/journal.pone.0100353)
15. Lowenstam HA. 1954 Factors affecting the aragonite: calcite ratios in carbonate-secreting marine organisms. *J. Geol.* **62**, 284–322. (doi:10.1086/626163)
16. Drenkard EJ, Cohen AL, McCorkle DC, de Putron SJ, Starczak VR, Zicht AE. 2013 Calcification by juvenile corals under heterotrophy and elevated CO_2. *Coral Reefs* **32**, 727–735. (doi:10.1007/s00338-013-1021-5)
17. Feely RA, Sabine CL, Hernandez-Ayon JM, Ianson D, Hales B. 2008 Evidence for upwelling of corrosive 'acidified' water onto the continental shelf. *Science* **320**, 1490–1492. (doi:10.1126/science.1155676)
18. Hofmann GE *et al.* 2014 Exploring local adaptation and the ocean acidification seascape—studies in the California Current Large Marine Ecosystem. *Biogeosciences* **11**, 1053–1064. (doi:10.5194/bg-11-1053-2014)
19. Feely RA, Alin SR, Carter B, Bednaršek N, Hales B, Chan F, Hill TM, Gaylord B, Sanford E, Byrne RH. 2016 Chemical and biological impacts of ocean acidification along the west coast of North America. *Estuarine, Coastal and Shelf Science* **183**, 260–270.
20. Washburn L, McPhee-Shaw E. 2013 Coastal transport processes affecting inner-shelf ecosystems in the California Current System. *Oceanography* **26**, 34–43. (doi:10.5670/oceanog.2013.43)
21. Gruber N, Hauri C, Lachkar Z, Loher D, Frolicher TL, Plattner GK. 2012 Rapid progression of ocean acidification in the California Current System. *Science* **337**, 220–223. (doi:10.1126/science.1216773)
22. Gaylord B *et al.* 2015 Ocean acidification through the lens of ecological theory. *Ecology* **96**, 3–15. (doi:10.1890/14-0802.1)
23. McKinney FK, Jackson JBC. 1989 *Bryozoan evolution*. Boston, UK: Unwin Hyman.
24. Hughes DJ. 1986 Life history variation in *Celleporella hyalina* (Bryozoa). *Proc. R. Soc. Lond. B* **228**, 127–132. (doi:10.1098/rspb.1986.0046)
25. Pistevos JCA, Calosi P, Widdicombe S, Bishop JDD. 2011 Will variation among genetic individuals influence species responses to global climate change? *Oikos* **120**, 675–689. (doi:10.1111/j.1600-0706.2010.19470.x)
26. Smith AM, Key MM, Gordon DP. 2006 Skeletal mineralogy of bryozoans: taxonomic and temporal patterns. *Earth Sci. Rev.* **78**, 287–306. (doi:10.1016/j.earscirev.2006.06.001)
27. Taylor PD, James NP, Bone Y, Kuklinski P, Kyser TK. 2009 Evolving mineralogy of cheilostome bryozoans. *Palaios* **24**, 440–452. (doi:10.2110/palo.2008.p08-124r)
28. Taylor PD, Lombardi C, Cocito S. 2015 Biomineralization in bryozoans: present, past and future. *Biol. Rev.* **90**, 1118–1150. (doi:10.1111/brv.12148)
29. Taylor PD, Monks N. 1997 A new cheilostome bryozoan genus pseudoplanktonic on molluscs and algae. *Invertebr. Biol.* **116**, 39–51. (doi:10.2307/3226923)

30. Soulé DF, Soulé JD, Chaney HW, Blake J, Scott P, Lissner A. 2005 *Taxonomic atlas of the benthic fauna of the Santa Maria Basin and Western Santa Barbara Channel:* vol. 13, *The Bryozoa*. Santa Barbara, CA: Santa Barbara Museum of Natural History.
31. Mercado JM, Carmona R, Niell FX. 1998 Bryozoans increase available CO_2 for photosynthesis in *Gelidium sesquipedale* (Rhodophyceae). *J. Phycol.* **34**, 925–927. (doi:10.1046/j.1529-8817.1998.340925.x)
32. Hunter E, Hughes RN. 1993 The effect of cell concentration on colony growth and feeding in the bryozoan *Celleporella hyalina*. *J. Mar. Biol. Assoc. UK* **73**, 321–331. (doi:10.1017/S0025315400032884)
33. McGowan JA, Cayan DR, Dorman LM. 1998 Climate-ocean variability and ecosystem response in the Northeast Pacific. *Science* **281**, 210–217. (doi:10.1126/science.281.5374.210)
34. Bischoff WD, Bishop FC, Mackenzie FT. 1983 Biogenically produced magnesian calcite; inhomogeneities in chemical and physical properties; comparison with synthetic phases. *Am. Mineral.* **68**, 1183–1188.
35. Gordon DP. 1977 The aging process in bryozoans. In *Biology of bryozoans* (eds RM Woollacott, RL Zimmer), pp. 335–376. New York, NY: Academic Press.
36. Palumbi SR, Jackson JBC. 1983 Aging in modular organisms: ecology of zooid senescence in *Steginoporella* sp. (Bryozoa; Cheilostomata). *Biol. Bull.* **164**, 267–278. (doi:10.2307/1541144)
37. Rucker JB, Carver RE. 1969 A survey of the carbonate mineralogy of cheilostome Bryozoa. *J. Paleontol.* **43**, 791–799.
38. Joyce TM, Robbins P. 1996 The long-term hydrographic record at Bermuda. *J. Climate* **9**, 3121–3131. (doi:10.1175/1520-0442(1996)009<3121:TLTHRA>2.0.CO;2)
39. Reed CG. 1987 Phylum Bryozoa. In *Reproduction and development of marine invertebrates of the northern Pacific coast* (ed. MF Strathmann). Seattle, WA: University of Washington Press.
40. Schwaninger HR. 1999 Population structure of the widely dispersing marine bryozoan *Membranipora membranacea* (Cheilostomata): implications for population history, biogeography, and taxonomy. *Mar. Biol.* **135**, 411–423. (doi:10.1007/s002270050642)
41. Saunders MI, Metaxas A. 2009 Effects of temperature, size, and food on the growth of *Membranipora membranacea* in laboratory and field studies. *Mar. Biol.* **156**, 2267–2276. (doi:10.1007/s00227-009-1254-6)
42. Yorke AF, Metaxas A. 2011 Interactions between an invasive and a native bryozoan (*Membranipora membranacea* and *Electra pilosa*) species on kelp and *Fucus* substrates in Nova Scotia, Canada. *Mar. Biol.* **158**, 2299–2311. (doi:10.1007/s00227-011-1734-3)
43. Bednaršek N, Feely R, Reum J, Peterson B, Menkel J, Alin S, Hales B. 2014 *Limacina helicina* shell dissolution as an indicator of declining habitat suitability owing to ocean acidification in the California Current Ecosystem. *Proc. R. Soc. B* **281**, 20140123. (doi:10.1098/rspb.2014.0123)
44. García-Reyes M, Largier J. 2010 Observations of increased wind-driven coastal upwelling off central California. *J. Geophys. Res.* **115**, 849. (doi:10.1029/2009JC005576)
45. Sydeman W, García-Reyes M, Schoeman D, Rykaczewski R, Thompson S, Black B, Bograd S. 2014 Climate change and wind intensification in coastal upwelling ecosystems. *Science* **345**, 77–80. (doi:10.1126/science.1251635)
46. Wang D, Gouhier TC, Menge BA, Ganguly AR. 2015 Intensification and spatial homogenization of coastal upwelling under climate change. *Nature* **518**, 390–394. (doi:10.1038/nature14235)
47. Roemmich D, McGowan J. 1995 Climatic warming and the decline of zooplankton in the California Current. *Science* **267**, 1324. (doi:10.1126/science.267.5202.1324)
48. Di Lorenzo E, Miller AJ, Schneider N, McWilliams JC. 2005 The warming of the California Current System: dynamics and ecosystem implications. *J. Phys. Oceanogr.* **35**, 336–362. (doi:10.1175/JPO-2690.1)
49. Barth JA *et al.* 2007 Delayed upwelling alters nearshore coastal ocean ecosystems in the northern California current. *Proc. Natl Acad. Sci. USA* **104**, 3719–3724. (doi:10.1073/pnas.0700462104)
50. Bond NA, Cronin MF, Freeland H, Mantua N. 2015 Causes and impacts of the 2014 warm anomaly in the NE Pacific. *Geophys. Res. Lett.* **42**, 3414–3420. (doi:10.1002/2015GL063306)
51. Rykaczewski RR, Dunne JP. 2010 Enhanced nutrient supply to the California Current Ecosystem with global warming and increased stratification in an earth system model. *Geophys. Res. Lett.* **37**, L21606. (doi:10.1029/2010GL045019)
52. McCoy S, Pfister C. 2014 Historical comparisons reveal altered competitive interactions in a guild of crustose coralline algae. *Ecol. Lett.* **17**, 475–483. (doi:10.1111/ele.12247)